

Broadband Rectangular Microstrip Antenna with Slits for W-Band Applications

AbdulGuddoos S. A. Gaid

Faculty of Engineering and Information Technology, Taiz University, Taiz, Yemen
quddoos.gaid@taiz.edu.ye

Mohammed A. E. Abdullah

Faculty of Engineering and Information Technology, Taiz University, Taiz, Yemen
Mohammed.abdullah.std@taiz.edu.ye

Mohammed M. S. Qaid

Faculty of Engineering and Information Technology, Taiz University, Taiz, Yemen
mohammedalwhapi2@gmail.com

Mohammad Ahmed Alomari

Faculty of Technology & Electronic and Computer Engineering, Universiti Teknikal Malaysia Melaka, Durian Tunggal, Melaka, Malaysia
alomari@utem.edu.my

Majid Khalaf Alshammari

School of Educational Studies, Universiti Sains Malaysia, Penang, Malaysia
m.alnehait@hotmail.com

Amer Sallam

Faculty of Engineering and Information Technology, Taiz University, Taiz, Yemen
Amer.sallam@taiz.edu.ye

Badiea Abdulkarem Mohammed

College of Computer Science and Engineering, University of Hail, Hail, Saudi Arabia
b.alshaibani@uoh.edu.sa (corresponding author)

Received: 28 November 2024 | Revised: 26 December 2024 | Accepted: 2 January 2025

Licensed under a CC-BY 4.0 license | Copyright (c) by the authors | DOI: <https://doi.org/10.48084/etasr.9759>

ABSTRACT

This work introduces a broadband rectangular patch antenna optimized for efficient data transmission in the W-band, particularly for 5G applications. By integrating two I-shaped slits with the radiating element, the antenna achieves an impressive performance, exhibiting wide bandwidth and excellent radiation characteristics. Utilizing Rogers RT5880 as the substrate material with a relative permittivity (ϵ_r) of 2.2, a small antenna with a size of $3.7 \times 4.1 \times 0.16 \text{ mm}^3$ is realized. Extensive simulations are conducted using CST software in both frequency and time domains to optimize the antenna. The results show a notable 16% fractional bandwidth from 80.75 GHz to 94.79 GHz, with dual resonance frequencies at 84.5 GHz and 91.5 GHz, primarily a result of the incorporated slits. At 84.5 GHz, the antenna demonstrates an outstanding reflection coefficient of -66.37 dB, a Voltage Standing Wave Ratio (VSWR) of 1.00096, a gain of 9.71 dBi, a directivity of 9.75 dB, and a high radiation efficiency of 91.8%. Similar trends are observed at 91.5 GHz, where the return loss remains at an impressive value of 55.92 dB and the VSWR maintains a very low value of 1.0032, indicating continued excellent impedance matching. While the gain (6.98 dBi) and directivity (7.05 dB) are slightly lower at this frequency, the radiation efficiency remains remarkably high at 94.9%, indicating efficient energy utilization. The wide bandwidth of the proposed design enables high data transfer rates, a crucial requirement for 5G networks. This translates to significant improvements in

network capacity, allowing for more connected devices and data traffic. Additionally, the design exhibits excellent signal transmission characteristics, ensuring reliable data transfer. Finally, the antenna's compact size and efficient radiation have the potential to reduce power consumption in 5G devices, contributing to improved battery life and sustainability.

Keywords-w-band; mm-wave; rectangular patch antenna; 5G networks; CST; high-speed transmission

I. INTRODUCTION

The development of fifth generation (5G) networks is a testament to the rapid progress of wireless communications technology. 5G boasts data rates that exceed those of 4G networks by a factor of 100. This leap is attributed to the utilization of the vast spectrum available in millimeter-wave (mmWave) bands. 5G networks have significantly enhanced universal connectivity and communication capacity, paving the way for high-speed data transmission and reduced latency. Furthermore, the integration of 5G with the Internet of Things (IoT) is now a reality [1-4].

To support the development of 5G, the Federal Communications Commission (FCC) has allocated the W-band (75-110 GHz) within the millimeter-wave spectrum (30-300 GHz) for 5G communications and its applications. With its short wavelengths and minimal atmospheric absorption loss, the W-band emerges as an exceptionally appealing domain for future advancement. These frequency ranges hold great promise for diverse wireless applications ranging from high-speed wireless communication networks, backhauling, precision radars, surveillance systems, high-resolution imaging, and biomedical applications [5-9].

In contemporary communication systems, antennas play a critical role and require enhanced attributes such as compactness, broad bandwidth, high gain, and effective radiation properties to accommodate the demanding 5G frequency bands. Microstrip antenna technology has attracted the interest of designers due to its slim profile, reliability, affordability, and seamless integration into confined spaces. Nevertheless, microstrip antennas still encounter gain and bandwidth hurdles that require further improvements [10-11].

Several studies have explored solutions to overcome the limitations of millimeter-wave antenna design, such as small bandwidth and poor gain [12-23]. The design suggested in [12] describes a rectangular patch antenna with square apertures, integrated into the upper layer of the antenna, for single-band operation. It operates between 64.20 GHz and 77.45 GHz, with a specific resonance at 73.7 GHz. The antenna is fabricated on a Rogers RT/Duroid 5880 substrate with a compact size (5.8 mm x 7.3 mm²) and specific properties: 0.55 mm substrate thickness, relative permittivity of 2.2, and loss tangent of 0.0009. The antenna offers an impedance bandwidth of 13.25 GHz, which is approximately 17.95% of the center frequency. It achieves good impedance matching with a Voltage Standing Wave Ratio (VSWR) of 1.02 and a reflection coefficient of -39.9 dB. Additionally, the antenna provides a peak gain of 6.08 dB at the center frequency. A tri-band antenna design is presented in [13]. This antenna targets three specific frequencies: 60 GHz, 94 GHz, and 110 GHz, covering a wide range from 52 GHz to 111 GHz. It achieves return loss values of 22.92 dB, 11.66 dB, and 22.16 dB at these frequencies,

respectively. It is important to note that the VSWR remains below 1.2 at both 60 GHz and 110 GHz, indicating good impedance matching at these points. However, at 94 GHz, the VSWR increases to 1.8, suggesting less than ideal impedance matching at this frequency. Additionally, the antenna delivers gains of 4.51 dB, 4.36 dB, and 6.03 dB at the respective resonant frequencies. Authors in [14] describe an E-band Y-shaped antenna. This antenna resonates at 76 GHz and covers a wide spectrum ranging from 70.98 GHz to 87.23 GHz. It offers a maximum gain of 8.77 dBi and a substantial impedance bandwidth of 16.25 GHz. The antenna is built on a Rogers RT-3003 material with a dielectric constant of 3, a loss tangent of 0.0013, and a thickness of 0.508 mm. The overall size of the antenna is $4.8 \times 5 \times 0.508$ mm³. Moreover, authors in [15] introduce a compact multi-band mmWave antenna design using a cost-effective Rogers RT/Duroid-5880 substrate. This design achieves five distinct impedance bandwidths suitable for mmWave applications (23.8 GHz, 39.4 GHz, 66.2 GHz, 81.9 GHz, and 93.9 GHz) while exhibiting promising gain values (6.18 - 7.7 dBi). The study reported in [16] proposes a dual-band antenna for mmWave applications (35.79 GHz & 72.71 GHz) with wide bandwidths (10.44 GHz & 6.71 GHz) and good radiation gains (8.01 dBi & 8.52 dBi). The antenna is constructed on a Rogers RT/Duroid-5880 substrate with a size of $7.18 \times 8.38 \times 0.78$ mm³ for optimal performance. In [17], a compact multiband antenna is presented, resonating at four distinct frequencies: 35.68 GHz, 45.2 GHz, 55.42 GHz, and 80.55 GHz. At these frequencies, it achieves return losses of 16.53 dB, 25.4 dB, 15.27 dB, and 22.7 dB, indicating robust signal transmission. Correspondingly, the antenna delivers peak gains of 4.76 dBi, 6.21 dBi, 7.58 dBi, and 5.97 dBi at these resonant points. The antenna spans a total impedance bandwidth of 16.8 GHz across these bands. It is constructed on a low-cost FR4 substrate with a permittivity of 4.3, a thickness of 1.6 mm, and a loss tangent of 0.025. The overall dimensions of the antenna are $5.5 \times 5.2 \times 1.6$ mm³. Authors in [18] introduce a single-band microstrip antenna with a dielectric constant of 2.2. This antenna is fabricated on a Rogers RT/Duroid5880 substrate with a thickness of 0.149 mm. To ensure proper impedance matching, an inset feed technique is employed between the feed microstrip line and the rectangular radiating patch. The antenna's dimensions are $2.02 \times 2.328 \times 0.149$ mm³, and it operates within the frequency range of 81.3717 GHz to 84.4912 GHz, with a center frequency of 83 GHz, providing an impedance bandwidth of 3.12 GHz. It boasts an impressive gain of 7.9087 dBi, a VSWR of 1.0033, and a return loss of 55.79 dB. A compact tri-band antenna design is presented in [19]. This antenna measures $8 \times 8.5 \times 0.508$ mm³ and operates efficiently at three distinct frequencies: 28 GHz, 38 GHz, and 60 GHz. Constructed on a Rogers RT/Duroid-5880 substrate, it achieves minimal signal reflection across these bands, as indicated by S_{11} values below -15 dB. Additionally, the antenna exhibits promising bandwidths at each operating frequency, with a particularly

notable bandwidth of 12.015 GHz at 60 GHz. Furthermore, it demonstrates encouraging signal strength (gains between 6.82 dBi and 7.96 dBi) and exceptional radiation efficiencies reaching up to 90%, indicating effective signal transmission. The design in [20] is a compact, multi-band antenna targeting W-band and D-band applications. This FR4-based design prioritizes affordability ($\epsilon_r = 4.3$, $\tan\delta = 0.025$) and maintains a small size ($4.8 \times 5.4 \times 1.6 \text{ mm}^3$). Notably, it resonates at five distinct frequencies (35.84 GHz, 46.07 GHz, 56.74 GHz, 81.6 GHz, and 110.09 GHz). The antenna exhibits impressive bandwidths, particularly at higher frequencies (3.3 GHz and 10.01 GHz for 81.6 GHz and 110.09 GHz, respectively). Additionally, it achieves promising gain values (6.22 dB and 8.51 dB) and excellent radiation efficiencies (94.06% and 93.52%) in these higher bands. Authors in [21] investigate a multi-band antenna design featuring an H-shaped radiating patch with an inset feed and a rectangular slit. The antenna is constructed on a Rogers RT/Duroid-5880 substrate ($\epsilon_r = 2.2$, $\tan\delta = 0.0009$, $7.5 \times 8.5 \times 0.55 \text{ mm}^3$) and resonates at five distinct frequencies: 23.2 GHz, 40.3 GHz, 59.3 GHz, 86.9 GHz, and 104.3 GHz. It exhibits bandwidths of 1.1 GHz, 2.8 GHz, 18.1 GHz, 7.7 GHz, and 10.7 GHz at these frequencies. The antenna also shows promising gain values ranging from 6.49 dBi to 9.82 dBi and achieves return loss values exceeding 19 dB at all resonant frequencies, with an especially low value of 2.25 dB at 104.3 GHz. Authors in [22] introduce a seven-band rectangular microstrip antenna featuring dual rectangular apertures. The antenna resonates at seven distinct frequencies (28.1 GHz - 82 GHz) with varying bandwidths (0.52 GHz - 3.09 GHz) and achieves good return loss across bands. Notably, it exhibits promising gain values, particularly at higher frequencies (7.17 dB at 60 GHz). Authors in [23] introduce a dual-band rectangular microstrip antenna designed to operate at 60 GHz and 93.7 GHz. This compact antenna has dimensions of $3.26 \times 3.94 \times 0.1 \text{ mm}^3$ and is built on a Rogers RT5880 substrate with a dielectric constant of 2.2, a loss tangent of 0.0009, and a thickness of 0.1 mm. It achieves bandwidths of 1.2 GHz at 60 GHz and 1.1 GHz at 93.7 GHz. The antenna also shows promising gain values of 6.67 dBi and 6.88 dBi, and effective signal transmission is indicated by return losses of 14.34 dB and 12.03 dB. Additionally, the VSWR values of 1.475 and 1.6682 at the respective resonant frequencies ensure proper impedance matching.

This study presents a simple, single-layer rectangular microstrip patch antenna design featuring two I-shaped slits, specifically tailored for W-band millimeter-wave applications. The proposed antenna combines high gain, wide bandwidth, excellent return loss, and high radiation efficiency, all within a compact and efficient form factor. Its compact size makes it well suited for integration into small 5G mobile devices operating in the W-band, while its superior return loss, high gain, and efficiency make it an excellent choice for low-power systems. Additionally, the design prioritizes simplicity and manufacturability by avoiding intricate geometries and sharp slots. By surpassing existing designs in gain and return loss, this antenna emerges as a highly promising candidate for future millimeter-wave wireless networks and low-power applications requiring compact and efficient antennas.

II. ANTENNA DESIGN METHODOLOGY

High-performance microstrip antenna design requires careful selection of parameters affecting bandwidth, gain, and efficiency. This study proposes a comprehensive, multi-stage approach. First, the initial antenna dimensions are derived from established formulas [24] for design accuracy. Second, a low-loss substrate such as Rogers RT5880 ($\epsilon_r = 2.2$, $\tan\delta = 0.0009$) is chosen to maximize efficiency. Critically, the substrate dimensions must exactly match the patch for optimal performance. The design process begins with the establishment of a baseline structure through simulation and initial design. Iterative optimization based on simulation results refines the design to achieve the desired specifications, allowing exploration of various configurations. Finally, the strategic introduction of slits or modifications can further enhance performance.

Material selection is critical. Rogers RT5880 minimizes signal loss due to its favorable dielectric properties. The iterative design process involves refining the antenna through adjustments based on simulations to achieve the desired performance. These adjustments can include the strategic introduction of slits or modifications to improve return loss, resonant frequency, and bandwidth.

Developing the antenna follows a structured four-stage process. Initially, the antenna has no slits (Figure 1(a)). If the calculated dimensions lead to an undesired resonant frequency, the patch length is adjusted (lengthening lowers frequency, shortening increases it) for precise calibration. Subsequent refinements aim to enhance performance. Introducing a single I-shaped slit on the left side of the patch (Figure 1(b)) improves return loss and alters the resonant frequency (84.2 GHz) for better resonance. Additionally, a new frequency band around 96.8 GHz provides expanded bandwidth.

Adding a second, I-shaped slit on the opposite side (Figure 1(c)) further improves return loss at two resonant frequencies and broadens the bandwidth. Finally, incorporating two identical I-shaped slits (Figure 1(d)) results in a broader operational band with improved return loss values. The expanded bandwidth (80.75 GHz to 94.79 GHz) highlights the effectiveness of this optimized design. Details on the final design, S_{11} performance comparisons, and optimal dimensions are shown in Figures 2, 3, and Table I.

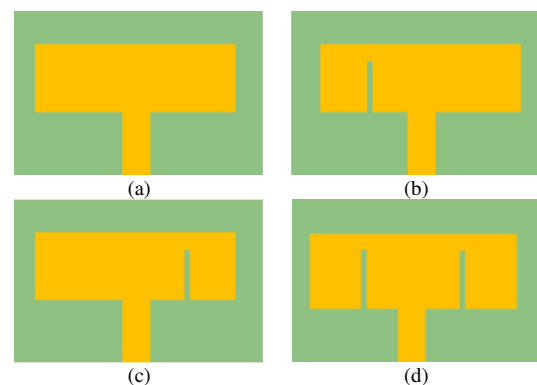


Fig. 1. Different configurations of the proposed antenna.

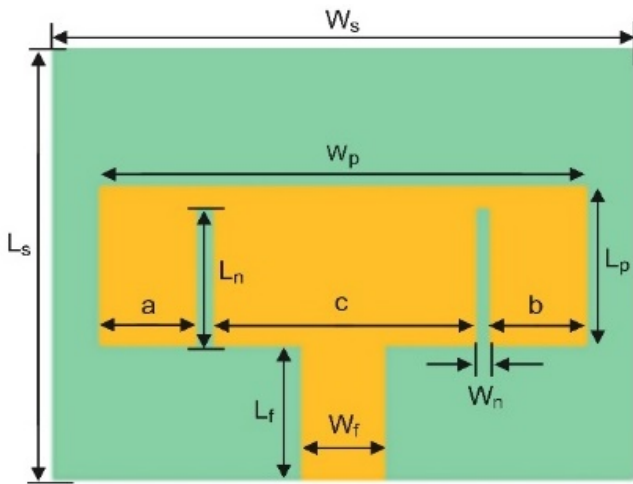


Fig. 2. The optimized design.

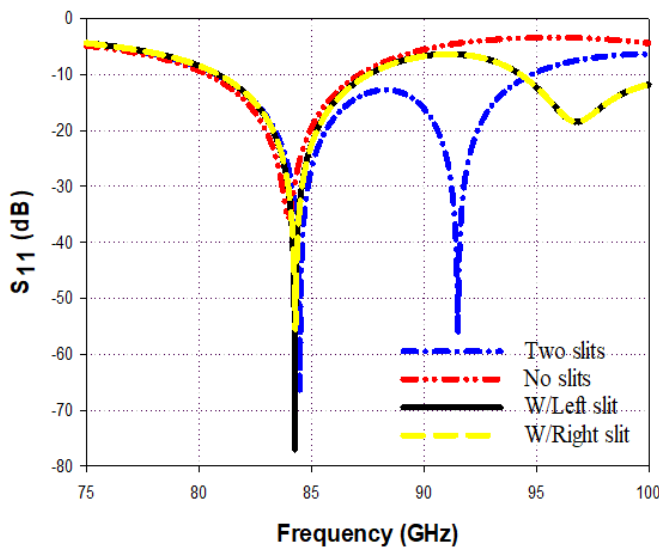


Fig. 3. S₁₁ performance for different antenna configurations.

TABLE I. THE OPTIMAL ANTENNA DIMENSIONS

Parameter	Symbol	Value (mm)
Width of the ground plane	W_s	4.1
Length of the ground plane	L_s	3.37
The substrate height	H_s	0.16
Width of the patch	W_p	3.5
Length of the patch	L_p	1.043
Width of the feed line	W_f	0.46
Length of the feed line	L_f	1.21
Length of the slit	L_n	0.951
Width of the slit	W_n	0.118
Left slit position	a	0.86
Right slit position	b	0.86
Distance between slits	c	1.544

III. PARAMETRIC ANALYSIS

In the course of developing the proposed antenna, five parameters are investigated to assess their influence on the S₁₁ performance. This section focuses on the analysis of the

positioning of the I-shaped slits in relation to the edges of the radiating patch and in relation to each other. Furthermore, the investigation extends to exploring the effects of the slit dimensions, including their lengths and widths.

A. Effects of the Slit Length

One of the parameters considered for analyzing its impact on the S₁₁ performance is the slit length (L_n). Through simulation of three different slit lengths and subsequent comparison of the results, the findings are presented in Figure 4. It is evident that as L_n varies from 0.6 mm to 0.951 mm, there is an expansion of the bandwidth from 9.45 GHz at a single resonant frequency to 14.04 GHz at two resonant frequencies. Concurrently, the return loss improves from 34.79 dB at 84.87 GHz to 66.37 dB and 55.92 dB at 84.5 GHz and 91.5 GHz, respectively. These observations indicate that a longer slot contributes to a broader bandwidth and enhances impedance matching. However, when L_n is further extended to 0.99 mm, the bandwidth remains unaffected whereas the return loss values decrease to approximately 40 dB at both resonant frequencies. Thus, based on the results depicted in Figure 4, the optimal choice for the slit length is $L_n = 0.951$ mm.

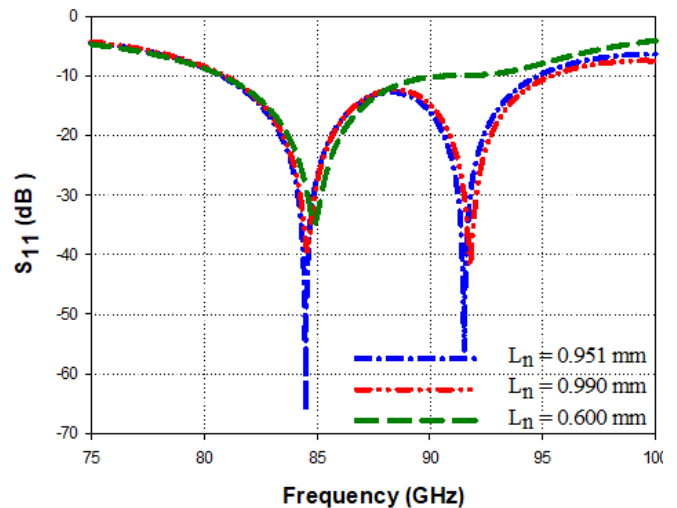


Fig. 4. S₁₁ performance for different values of slit length (L_n).

B. Effects of the Slit Width

Figure 5 illustrates the return loss performance for various values of the slit width (W_n). It is observed that the most optimal performance is achieved for $W_n = 0.118$ mm. At this specific width, the impedance bandwidth expands to 14.04 GHz, whereas the return loss values improve significantly to 66.37 dB and 55.92 dB at resonant frequencies of 84.5 GHz and 91.5 GHz, respectively. Additionally, it is noted that the slit width also affects the resonant frequencies. Specifically, there is a slight shift towards higher resonant frequencies when the slit width is increased from $W_n = 0.118$ mm to $W_n = 0.150$ mm. Conversely, decreasing the slit width to $W_n = 0.100$ mm results in a minor shift towards lower resonant frequencies. Moreover, deviations from the optimal slit width result in a reduction in return loss values at the upper resonant frequency.

C. Effects of the Left Slit Position

The effect of the left-side slit placement on return loss is illustrated in Figure 6. At a distance (a) of 0.76 mm, the antenna resonates at 83 GHz and 90.7 GHz, achieving return losses of 46 dB and 21 dB, respectively. As this distance increases to 0.95 mm, the resonant frequencies shift slightly to 84.9 GHz and 90 GHz, with corresponding return losses of 49 dB and 44 dB. Interestingly, a significant improvement in return loss is observed at a specific placement ($a = 0.86$ mm). In this configuration, the return loss reaches 66.37 dB and 55.92 dB at the respective resonant frequencies of 84.5 GHz and 91.5 GHz. Figure 6 clearly demonstrates the substantial improvement in return loss performance that can be achieved through optimal slit positioning.

D. Effects of the Right Slit Position

Figure 7 examines how the placement of the right-side slit relative to the patch edge affects the antenna's return loss (S_{11} performance). At a distance (b) of 0.82 mm, the antenna resonates at 84.1 GHz and 91.5 GHz with return losses of 54 dB and 29 dB, respectively. Increasing this distance to $b = 0.9$ mm causes a minor shift in the resonant frequencies to 84.7 GHz and 91 GHz. The corresponding return losses at these frequencies are 59 dB and 39 dB, respectively. Interestingly, a significant improvement in return loss is achieved at a specific placement ($b = 0.86$ mm) from the right edge. In this configuration, the return loss reaches 66.37 dB and 55.92 dB at the respective resonant frequencies of 84.5 GHz and 91.5 GHz. This figure underlines the importance of optimal slit positioning for maximizing return loss performance.

E. Effects of the Distance Between the Slits

Figure 8 examines the effect of varying the distance (c) between the two slits on the antenna's return loss performance. When the spacing is set to $c = 1.218$ mm, the antenna resonates at 84.6 GHz and 90.2 GHz, achieving return losses of 48 dB and 32 dB, respectively. Increasing the slit spacing to $c = 1.318$ mm slightly shifts the resonant frequencies to 84 GHz and 92 GHz. The corresponding return losses are 44 dB and 20 dB, respectively. Interestingly, a significant improvement in return loss is observed at a specific spacing ($c = 1.544$ mm). In this configuration, the return losses reach 66.37 dB and 55.92 dB at the respective resonant frequencies of 84.5 GHz and 91.5 GHz. This figure highlights the importance of optimizing the slit spacing to achieve the best return loss performance.

IV. SIMULATION RESULTS AND VALIDATION

This work utilizes CST simulation software (both frequency-domain and time-domain solvers) to explore the design of a compact rectangular microstrip patch antenna with dual slits. This antenna targets high-speed data transmission within the millimeter-wave band, specifically for potential use in 5G applications. The analysis carefully evaluates critical performance parameters, including resonant frequencies, return loss, VSWR, gain, directivity, and radiation efficiency. Current distribution, E-plane and H-plane radiation patterns are also examined. Table II summarizes the findings for the proposed antenna, demonstrating its strong performance and suitability for high-speed data transmission in 5G applications across various resonant frequencies.

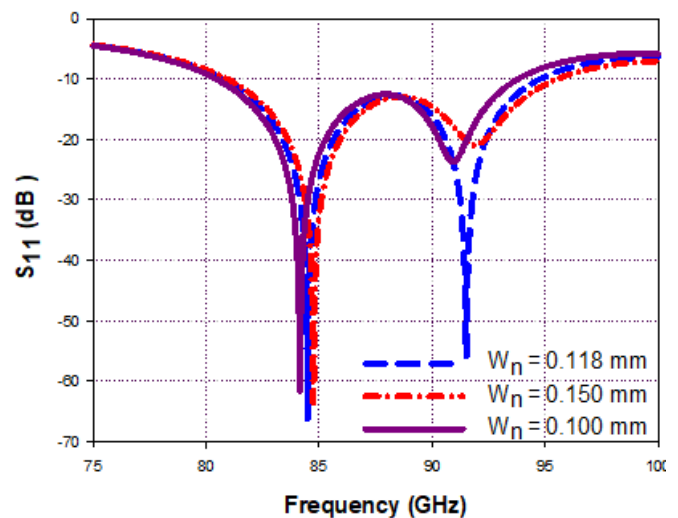


Fig. 5. S_{11} performance for different values of slit width (W_n).

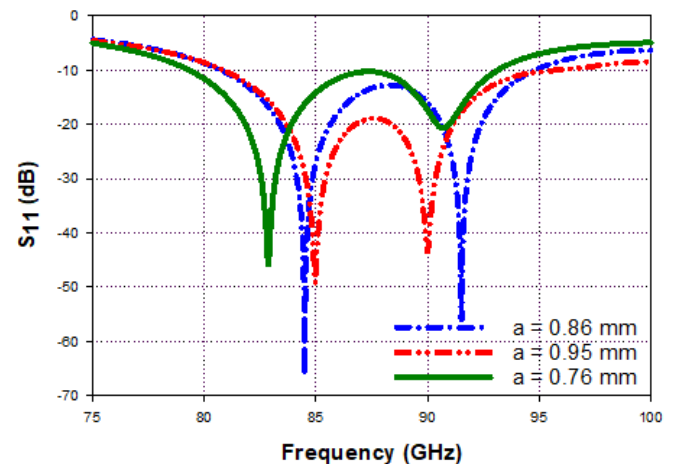


Fig. 6. S_{11} performance for different values of the left slit position (a).

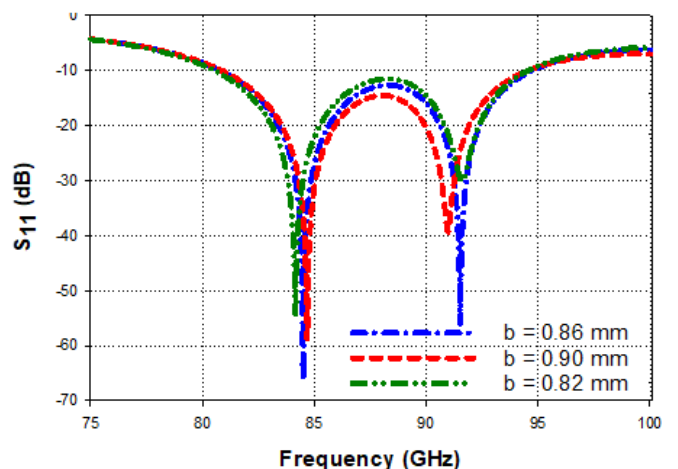


Fig. 7. S_{11} performance for different values of the right slit position (b).

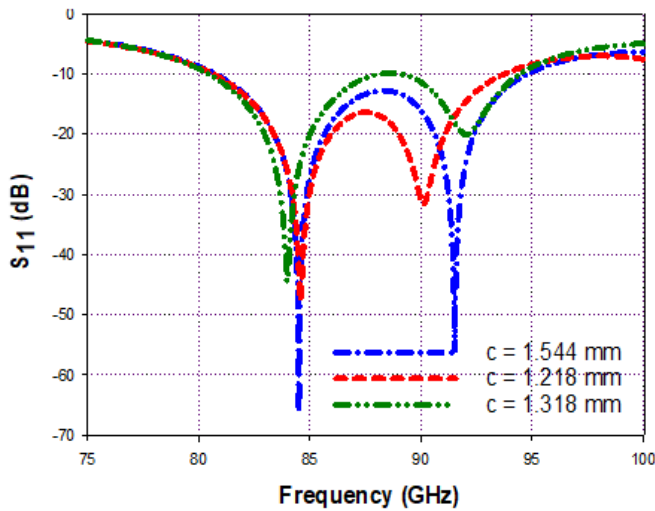


Fig. 8. S_{11} performance for different values of slit distance (c).

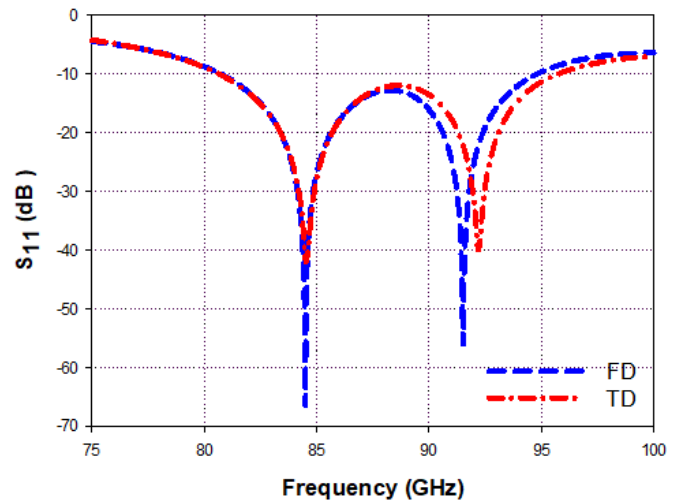


Fig. 9. S_{11} performance of the optimized antenna using CST (TD and FD).

A. The Return Loss Performance

Based on the analysis of simulated results obtained from CST in the Frequency Domain (FD), the antenna exhibits impressive return loss values at both resonant frequencies: 66.37 dB at 84.5 GHz and 55.92 dB at 91.5 GHz. These values indicate minimal signal reflection and efficient power transfer, essential qualities for high-performance antennas. Additionally, the achieved bandwidth ($S_{11} \leq -10$ dB) extends over 14.04 GHz, covering the frequency range from 80.75 to 94.79 GHz. These findings are confirmed by comparisons made using CST in the Time Domain (TD), as illustrated in Figure 9. Remarkably, there is excellent agreement between the frequency-domain and time-domain CST results, although slight frequency shifts are observed for the second resonant frequency and there is a relatively minor reduction in return losses at the resonant frequencies.

B. The VSWR Performance

Ensuring a low VSWR is vital for minimizing signal losses and guaranteeing efficient signal transmission. Figure 10 illustrates the simulated VSWR across operating frequencies obtained from CST in both the FD and the TD. The VSWR values are 1.00096 for the lower resonant frequency (84.5 GHz) and 1.0032 for the upper resonant frequency (91.5 GHz) as obtained with CST (FD). The subsequent assessment with CST (TD) verifies the alignment with the results obtained with CST (FD), as depicted in Figure 10.

C. Total and Radiation Efficiencies

The high efficiency highlights the antenna's effectiveness in converting input power into radiated energy. Figure 11 illustrates the total and radiation efficiencies across operational frequencies. The radiation efficiency is impressive, reaching 91.8% at the lower resonant frequency (84.5 GHz) and 94.9% at the upper resonant frequency (91.5 GHz). Furthermore, the radiation efficiency consistently surpasses 90% across the operational bandwidth, as shown in the figure. Similarly, the antenna's total efficiency exceeds 80% throughout the bandwidth.

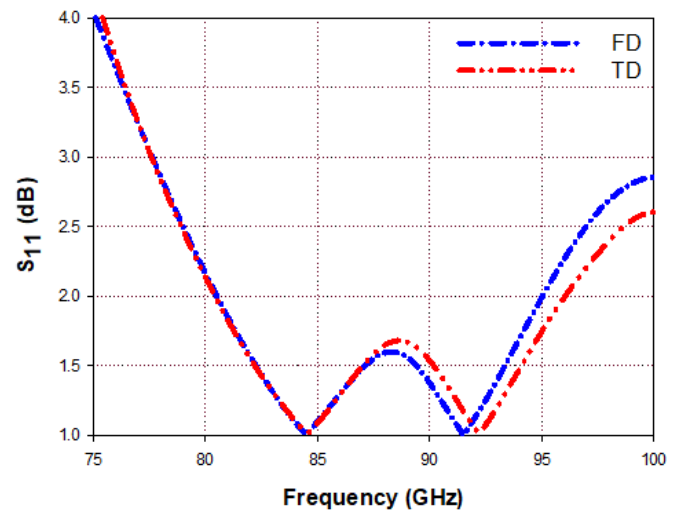


Fig. 10. VSWR performance of the optimized antenna using CST (TD and FD).

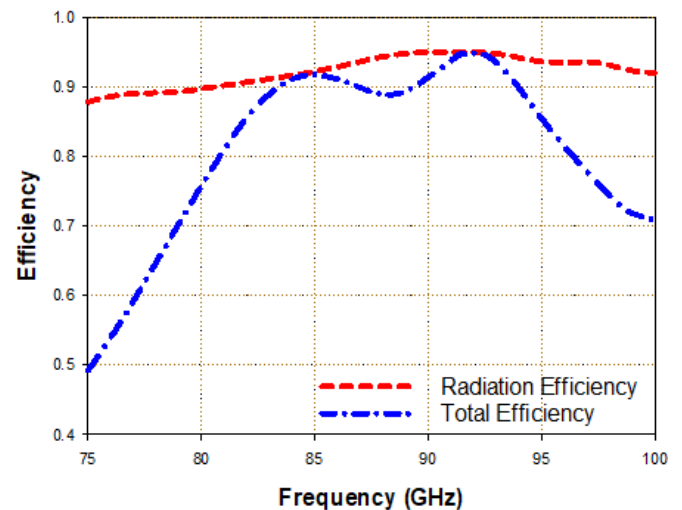


Fig. 11. Antenna efficiency vs the operational band.

D. Gain and Directivity

The antenna demonstrates significant gains and directivities, achieving a gain of 9.71 dBi and a directivity of 9.75 dB at the lower resonant frequency (84.5 GHz), as depicted in Figure 12(a). Conversely, at the upper resonant frequency (91.5 GHz), the gain decreases to 6.98 dBi, and the directivity decreases to 7.05 dB, as shown in Figure 12(b). These values highlight the antenna's ability to focus signals in specific directions, which is crucial for reliable communications and data transmission.

E. Surface Current Distribution

Analysis of the current distribution in the microstrip antenna reveals a significant concentration of current along the edge of the microstrip patch during resonance. The inclusion of two strategically positioned slits in the patch amplifies this distribution, resulting in enhanced current directionality and increased antenna efficiency. Furthermore, the results indicate a positive impact on the edges of the slits, which helps to direct the current along the feed line, as depicted in Figure 13. This comprehension of the underlying dynamics underscores the importance of slits in enhancing antenna performance and achieving an optimal current distribution across a microstrip patch.

F. Two Dimensional Radiation Patterns

Figure 14 shows the two-dimensional (2D) radiation patterns for both the E-plane and the H-plane. Figure 14(a) illustrates the E-plane at the lower resonant frequency (84.5 GHz), showcasing effective signal directionality. Additionally, Figure 14(b) exhibits the magnetic field (H-plane) at the same frequency, indicating a similar signal orientation. The antenna's gain can be approximated by reading the values from the 2D radiation patterns, typically close to 10 dBi. Similarly, Figure 15(a) shows the E-plane at the higher frequency (91.5 GHz), whereas Figure 15(b) illustrates the H-plane. The results in both planes are noteworthy. A comparison of the frequency and time domain results using CST software reveals excellent agreement, as demonstrated in the figures. This comprehensive analysis underscores the antenna's efficiency in achieving superior coverage and directionality across the operating band in both the E and H planes, thereby enhancing its suitability for high quality communications in these frequency bands.

G. Comparison with Other Published Works

Table III presents a comprehensive comparison between our proposed antenna and several designs found in the literature. The comparison includes various parameters such as overall size, impedance bandwidth, reflection coefficient (S_{11}), and gain. Our proposed design exhibits superior performance compared to all the designs listed in the table, especially in terms of gain, VSWR, and S_{11} . Although the design presented in [14] achieves a slightly wider bandwidth, our proposed design surpasses it in terms of gain, VSWR, and S_{11} . The designs presented in [18] and [23] are marginally smaller, but they fall short in impedance bandwidth, gain, VSWR, and S_{11} when compared to our proposed design.

TABLE II. RESULTS SUMMARY

Resonant frequency	$f_{r1} = 84.5$ GHz	$f_{r2} = 91.5$ GHz
S_{11} (dB)	66.37	55.92
VSWR	1.00096	1.0032
BW (GHz)	14.04	
Gain (dBi)	9.71	6.98
Directivity (dB)	9.75	7.05
Radiation efficiency (%)	91.8	94.9

TABLE III. COMPARATIVE ANALYSIS REVIEW

Ref.	[12]	[14]	[18]	[23]	This work
f_r (GHz)	73.7	76	83	60/93.7	84.5/91.5
Size (mm ³)	5.8x7.3x0.55	4.8x5x0.508	2.02x2.328x0.149	3.26x3.94x0.1	3.7x4.1x0.16
BW (GHz)	13.25	16.25	3.12	1.2/1.1	14.04
Gain (dBi)	6.08	8.77	7.9	6.67/6.88	9.71/6.98
S_{11} (dB)	-39.9	-20	-55.8	-14.34/-12.03	-66.37/-55.92
VSWR	1.02	-	1.003	1.48/1.67	1.001/1.003

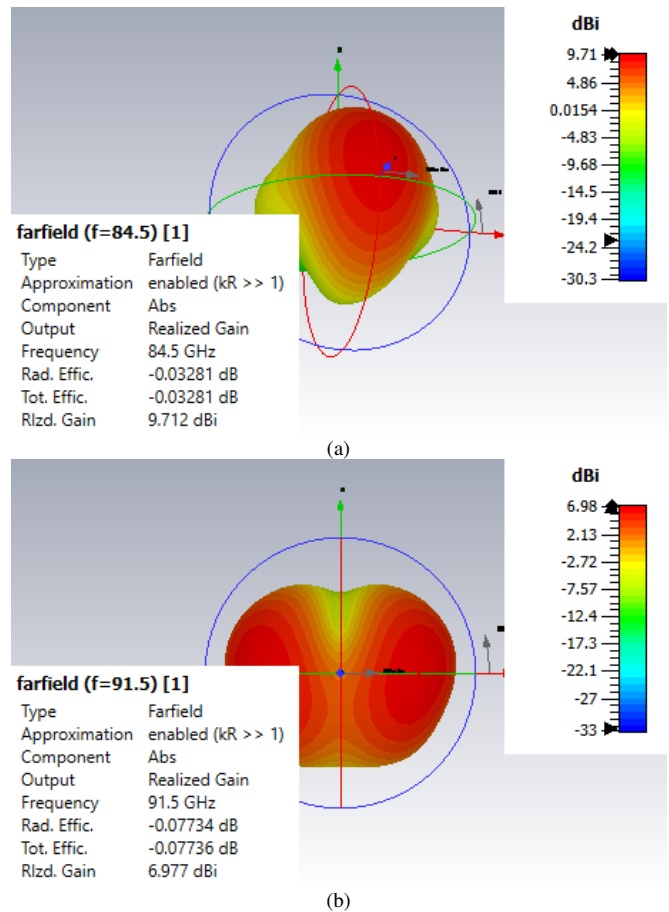


Fig. 12. Three dimensional radiation patterns at: (a) 84.5 GHz and (b) 91.5 GHz.

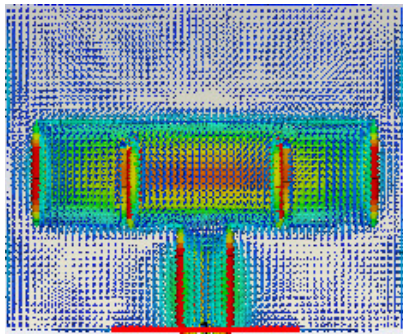


Fig. 13. The surface current distribution at 84.5 GHz.

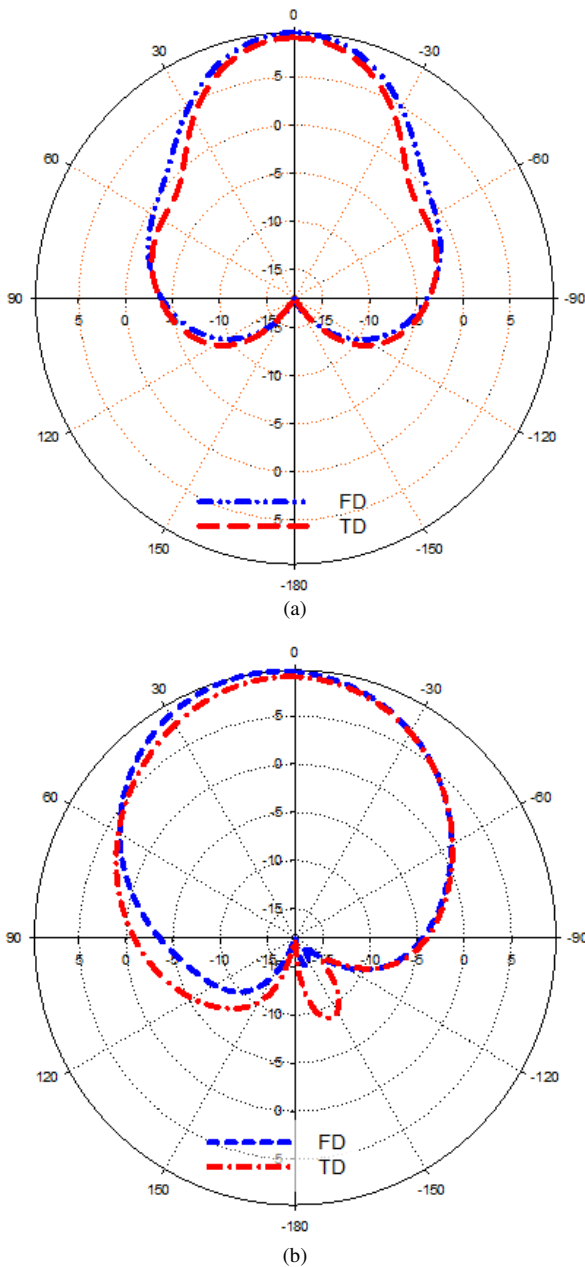


Fig. 14. Two dimensional radiation patterns at 84.5 GHz: (a) E-plane and (b) H-plane.

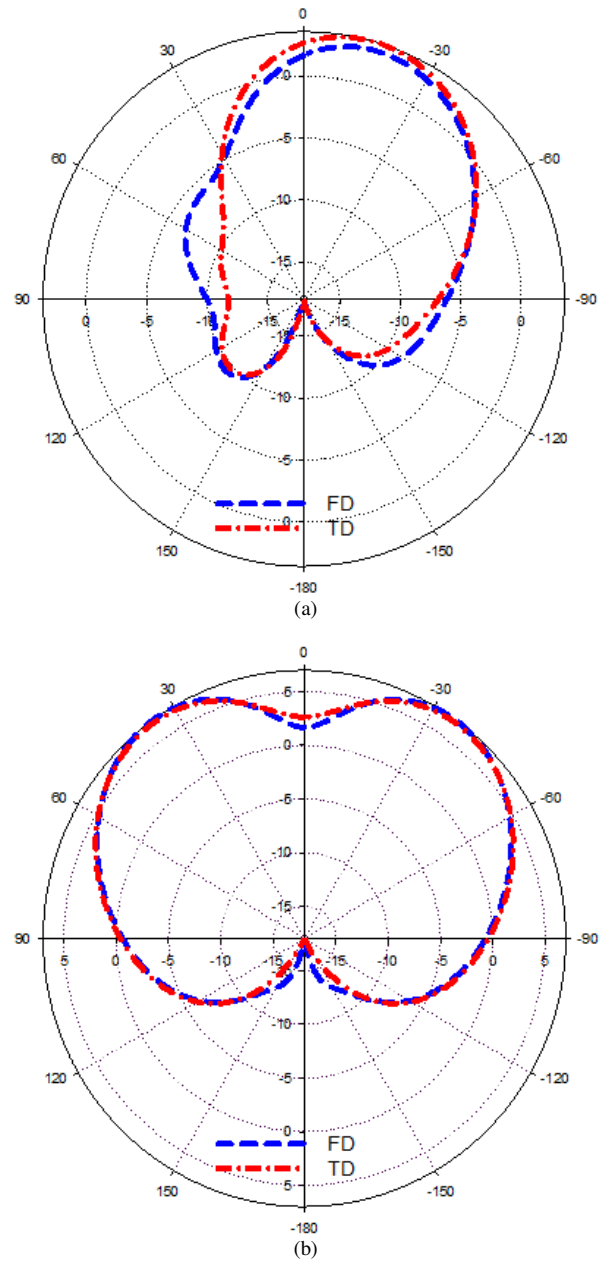


Fig. 15. Two dimensional radiation patterns at 91.5 GHz: (a) E-plane and (b) H-plane.

V. CONCLUSION

This study presents an enhanced rectangular patch antenna design that incorporates two identical I-shaped slits at its rear edge, leading to significant performance improvements, including wider bandwidth and higher return loss characteristics. Using a Rogers RT5880 substrate with tailored dimensions and properties, the antenna resonates at 84.5 GHz and 91.5 GHz, achieving a wide bandwidth of 14.04 GHz, spanning from 80.75 GHz to 94.79 GHz. At the first resonant frequency (84.5 GHz), the antenna demonstrates excellent performance with a high radiation gain of 9.71 dBi and a return loss of 66.37 dB, indicating exceptional impedance matching.

At the second resonant frequency (91.5 GHz), the antenna achieves a gain of 6.98 dBi and a return loss of 55.92 dB. Additionally, the radiation efficiencies at these frequencies are 91.8% and 94.9%, respectively. This design offers a promising solution for high-speed data transmission in 5G millimeter-wave communication systems, meeting the stringent demands of advanced wireless technologies. Future research could explore further optimization of slitted antenna designs to enhance performance and validate the proposed design through fabrication and experimental measurements.

REFERENCES

- [1] J. G. Andrews *et al.*, "What Will 5G Be?," *IEEE Journal on Selected Areas in Communications*, vol. 32, no. 6, pp. 1065–1082, Jun. 2014, <https://doi.org/10.1109/JSAC.2014.2328098>.
- [2] A. S. A. Gaid and M. A. M. Ali, "Design and Simulation of a Compact Microstrip Antenna for 5G Applications at the (37 – 40) GHz Band," *Journal of Nano- and Electronic Physics*, vol. 15, no. 4, Aug. 2023, Art. no. 04039, [https://doi.org/10.21272/jnep.15\(4\).04039](https://doi.org/10.21272/jnep.15(4).04039).
- [3] B. Bertenyi, "5G Evolution: What's Next?," *IEEE Wireless Communications*, vol. 28, no. 1, pp. 4–8, Feb. 2021, <https://doi.org/10.1109/MWC.2021.9363048>.
- [4] A. S. A. Gaid and A. N. S. Ali, "High-Gain Microstrip Patch Antenna with a Circular Slot for WiGig Applications in the V - Band," *Journal of Nano- and Electronic Physics*, vol. 16, no. 1, Feb. 2024, Art. no. 01001, [https://doi.org/10.21272/jnep.16\(1\).01001](https://doi.org/10.21272/jnep.16(1).01001).
- [5] S. Agarwal, N. P. Pathak, and D. Singh, "Concurrent 83GHz/94 GHz parasitically coupled defected microstrip feedline antenna for millimeter wave applications," in *2013 IEEE Applied Electromagnetics Conference*, Bhubaneswar, India, 2013, pp. 1–2, <https://doi.org/10.1109/AEMC.2013.7045120>.
- [6] G. Chittimoju and U. D. Yalavarthi, "A Comprehensive Review on Millimeter Waves Applications and Antennas," *Journal of Physics: Conference Series*, vol. 1804, no. 1, Feb. 2021, Art. no. 012205, <https://doi.org/10.1088/1742-6596/1804/1/012205>.
- [7] M. Anab, M. I. Khattak, S. M. Owais, A. A. Khattak, and A. Sultan, "Design and Analysis of Millimeter Wave Dielectric Resonator Antenna for 5G Wireless Communication Systems," *Progress In Electromagnetics Research C*, vol. 98, pp. 239–255, Jan. 2020, <https://doi.org/10.2528/PIERC19102404>.
- [8] J. Doo, W. Park, W. Choe, and J. Jeong, "Design of Broadband W-Band Waveguide Package and Application to Low Noise Amplifier Module," *Electronics*, vol. 8, no. 5, May 2019, Art. no. 523, <https://doi.org/10.3390/electronics8050523>.
- [9] Y. Zhang, A. R. Vilenskiy, and M. V. Ivashina, "W-band Waveguide Antenna Elements for Wideband and Wide-Scan Array Antenna Applications For Beyond 5G," in *2021 15th European Conference on Antennas and Propagation*, Dusseldorf, Germany, 2021, pp. 1–5, <https://doi.org/10.23919/EuCAP51087.2021.9411184>.
- [10] D. Imran *et al.*, "Millimeter wave microstrip patch antenna for 5G mobile communication," in *2018 International Conference on Engineering and Emerging Technologies*, Lahore, Pakistan, 2018, pp. 1–6, <https://doi.org/10.1109/ICEET1.2018.8338623>.
- [11] S. Palanivel Rajan and C. Vivek, "Analysis and Design of Microstrip Patch Antenna for Radar Communication," *Journal of Electrical Engineering & Technology*, vol. 14, no. 2, pp. 923–929, Mar. 2019, <https://doi.org/10.1007/s42835-018-00072-y>.
- [12] A. M. H. Aoun, A. A. A. Saeed, A. S. A. Gaid, O. Y. A. Saeed, M. N. G. Mohammed, and B. Hawash, "E-Band Slotted Microstrip Patch Antenna for 5G Mobile Backhaul Applications," in *2021 International Conference of Technology, Science and Administration*, Taiz, Yemen, 2021, pp. 1–5, <https://doi.org/10.1109/ICTSA52017.2021.9406550>.
- [13] A. Ahmed, H. M. Arifur Rahman, and M. M. Khan, "Design and Analysis of a Compact Wideband V-Band and W-Band Antenna for Healthcare Applications," in *2022 IEEE 12th Annual Computing and Communication Workshop and Conference*, Las Vegas, NV, USA, 2022, pp. 1043–1048, <https://doi.org/10.1109/CCWC54503.2022.9720767>.
- [14] W. A. Awan, A. Zaidi, N. Hussain, and A. Baghdad, "Compact Size Y-Shaped Broadband Antenna For E-Band Applications," in *2019 International Conference on Wireless Technologies, Embedded and Intelligent Systems*, Fez, Morocco, 2019, pp. 1–3, <https://doi.org/10.1109/WITS.2019.8723799>.
- [15] A. A. A. Saeed, O. Y. A. Saeed, A. S. A. Gaid, A. M. H. Aoun, and A. A. Sallam, "A low Profile Multiband Microstrip Patch Antenna For 5G Mm-Wave Wireless Applications," in *2021 International Conference of Technology, Science and Administration*, Taiz, Yemen, 2021, pp. 1–5, <https://doi.org/10.1109/ICTSA52017.2021.9406519>.
- [16] A. S. A. Gaid, A. A. Sallam, A. M. H. Aoun, A. A. A. Saeed, and O. Y. A. Saeed, "Dual Band Rectangular Microstrip Patch Antenna for 5G Millimeter-Wave Wireless Access and Backhaul Applications," in *Innovative Systems for Intelligent Health Informatics (IRICT 2020)*, F. Saeed, F. Mohammed, and A. Al-Nahari, Eds. Cham, Switzerland: Springer International Publishing, 2021, pp. 728–738.
- [17] A. K. Galib, N. Sarker, and M. R. H. Mondal, "Two Compact Multiband Millimetre Wave Antennas for Wireless Communication," in *2019 IEEE International Conference on Telecommunications and Photonics*, Dhaka, Bangladesh, 2019, pp. 1–4, <https://doi.org/10.1109/ICTP48844.2019.9041755>.
- [18] A. S. A. Gaid, S. M. E. Saleh, A. H. M. Qahtan, S. G. A. Aqlan, B. A. E. Yousef, and A. A. A. Saeed, "83 GHz Microstrip Patch Antenna for Millimeter Wave Applications," in *2021 International Conference of Technology, Science and Administration*, Taiz, Yemen, 2021, pp. 1–4, <https://doi.org/10.1109/ICTSA52017.2021.9406546>.
- [19] A. S. A. Gaid and M. A. M. Ali, "Tri-Band Rectangular Microstrip Patch Antenna with Enhanced Performance for 5G Applications Using a π -Shaped Slot: Design and Simulation," *Iraqi Journal for Electrical and Electronic Engineering*, vol. 19, no. 2, pp. 179–190, Dec. 2023, <https://doi.org/10.37917/ijeee.19.2.20>.
- [20] A. K. Galib, N. Sarker, and M. R. H. Mondal, "Novel Multiband Millimeter Wave Antennas," *Journal of Communications*, vol. 18, no. 1, pp. 1–14, Jan. 2023, <https://doi.org/10.12720/jcm.18.1.1-14>.
- [21] O. Y. A. Saeed, A. A. A. Saeed, A. S. A. Gaid, A. M. H. Aoun, and A. A. Sallam, "Multiband Microstrip Patch Antenna Operating at Five Distinct 5G mm-Wave Bands," in *2021 International Conference of Technology, Science and Administration*, Taiz, Yemen, 2021, pp. 1–5, <https://doi.org/10.1109/ICTSA52017.2021.9406521>.
- [22] W. Shahjehan, I. Hussain, K. Amin, I. Ali, A. Riaz, and P. Uthansakul, "Hepta-Band Antenna for 5G Applications," *Wireless Personal Communications*, vol. 125, no. 3, pp. 2031–2054, Aug. 2022, <https://doi.org/10.1007/s11277-022-09644-8>.
- [23] S. D. Sateaa, M. S. Hussein, Z. G. Faisal, A. M. Abood, and H. D. Sateaa, "Design and simulation of dual-band rectangular microstrip patch array antenna for millimeter-wave," *Bulletin of Electrical Engineering and Informatics*, vol. 11, no. 1, pp. 299–309, Feb. 2022, <https://doi.org/10.11591/eei.v11i1.3336>.
- [24] A. S. A. Gaid, M. A. M. Ali, A. Saif, and W. A. A. Mohammed, "Design and analysis of a low profile, high gain rectangular microstrip patch antenna for 28 GHz applications," *Cogent Engineering*, vol. 11, no. 1, Dec. 2024, Art. no. 2322827, <https://doi.org/10.1080/23311916.2024.2322827>.